European Journal of Medicinal Chemistry 80 (2014) 122–134

Contents lists available at ScienceDirect

European Journal of Medicinal Chemistry

journal homepage: http://www.elsevier.com/locate/ejmech

Original article

Polycyclic propargylamine and acetylene derivatives as multifunctional neuroprotective agents

Frank T. Zindo [a], Quinton R. Barber [b], Jacques Joubert [a], Jacobus J. Bergh [b], Jacobus P. Petzer [b], Sarel F. Malan [a,b,*]

[a] Pharmaceutical Chemistry, School of Pharmacy, University of The Western Cape, Private Bag X17, Bellville 7535, South Africa
[b] Pharmaceutical Chemistry, North-West University, Private Bag X6001, Potchefstroom 2520, South Africa

ARTICLE INFO

Article history:
Received 10 December 2013
Received in revised form
2 April 2014
Accepted 11 April 2014
Available online 13 April 2014

Keywords:
Polycyclic
Propargylamine
Neuroprotection
Apoptosis

ABSTRACT

The aim of this study was to design drug-like molecules with multiple neuroprotective mechanisms which would ultimately inhibit *N*-methyl-D-aspartate (NMDA) receptors, block *L*-type voltage gated calcium channels (VGCC) and inhibit apoptotic processes as well as the monoamine oxidase-B (MAO-B) enzyme in the central nervous system. These types of compounds may act as neuroprotective and symptomatic drugs for disorders such as Alzheimer's and Parkinson's disease. In designing the compounds we focused on the structures of rasagiline and selegiline, two well known MAO-B inhibitors and proposed neuroprotective agents. Based on this consideration, the compounds synthesised all contain the propargylamine functional group of rasagiline and selegiline or a derivative thereof, conjugated to various polycyclic cage moieties. Being non-polar, these polycyclic moieties have been shown to aid in the transport of conjugated compounds across the blood–brain barrier, as well as cell membranes and have secondary positive neuroprotective effects. All novel synthesised polycyclic derivatives proved to have significant anti-apoptotic activity ($p < 0.05$) which was comparable to the positive control, selegiline. Four compounds (**12**, **15** and **16**) showed promising VGCC and NMDA receptor channel inhibitory activity ranging from 18% to 59% in micromolar concentrations and compared favourably to the reference compounds. In the MAO-B assay, 8-phenyl-ethynyl-8-hydroxypentacycloundecane (**10**), exhibited MAO-B inhibition of 73.32% at 300 μM. This compound also reduced the percentage of apoptotic cells by as much as 40% when compared to the control experiments.

1. Introduction

The pathology of neurodegenerative disorders, such as Parkinson's disease (PD) and Alzheimer's disease (AD), is caused by the abnormal loss of neuronal cells in certain areas of the brain [1]. It consequently causes an imbalance of certain neurotransmitter levels in the brain, giving rise to the characteristic signs and symptoms of these disorders [2,3]. Ultimately, it compromises the normal functionality and well-being of the individual suffering from the disease [3], thus making it an absolute necessity to create drugs which would halt this neuronal breakdown process and aid in treating the signs and symptoms of neurodegenerative disorders. The abnormal death of neurons in the central nervous system of individuals suffering from neurodegenerative diseases takes place by an intrinsic cell suicide program known as apoptosis [4–7]. This process is triggered by several stimuli, and consists of numerous pathways and cascades, each one having an influence on the other, ultimately leading to cell death [4–7]. One such pathway is the excitotoxic process which leads to apoptosis. Excitotoxicity is a result of activation of postsynaptic receptors; including NMDA receptors, 2-amino-3-(3-hydroxy-5-methylisoxazol-4-yl) propionate (AMPA), and kainate receptors. Upon their activation, these receptors open their associated ion channel to allow the influx of Ca^{2+} and Na^{+} ions. The excessive influx of calcium together with any calcium release from intracellular compartments can overwhelm Ca^{2+}-regulatory mechanisms and lead to cell death [8,9]. This mechanism of cell death suggests that the receptors and their associated calcium channels serve as drug target sites for curbing neurodegeneration. Several compounds, including polycyclic amines such as amantadine (**2**), NGP1-01 (**3**), MK-801 (**4**), and phencyclidine (PCP, **5**) have been reported to show inhibitory activities on NMDA receptors and calcium channels (Fig. 1) [10].

* Corresponding author. Present address: School of Pharmacy, University of the Western Cape, Private Bag X17, Bellville 7535, South Africa.
E-mail address: sfmalan@uwc.ac.za (S.F. Malan).

http://dx.doi.org/10.1016/j.ejmech.2014.04.039
0223-5234/

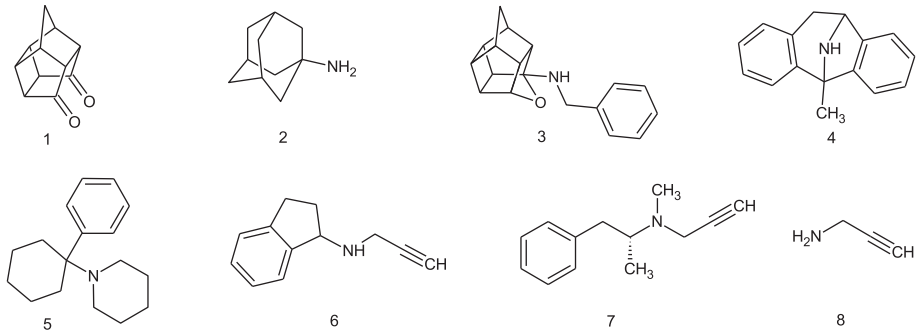

Fig. 1. Representative polycyclic cage compounds (**1**–**3**), NMDA receptor and calcium channel modulators - NGP1-01 (**3**), MK-801 (**4**) and phencyclidine (PCP, **5**), the neuroprotective MAO-B inhibitors - rasagiline (**6**) and selegiline (7), and propargylamine (**8**).

The oxidative deamination reaction catalysed by monoamine oxidase-B (MAO-B) is one of the major catabolic pathways of dopamine in the brain. Inhibition of this enzyme lead to enhanced dopaminergic neurotransmission and is currently used in the symptomatic treatment of PD [11–14]. Furthermore, MAO-B inhibitors may also exert a neuroprotective effect by reducing the concentrations of potentially hazardous by-products produced by MAO-B-catalysed dopamine oxidation [15]. In PD and AD it has been shown that there are age-related elevated levels of MAO-B, which not only act indirectly as a trigger to the apoptotic process, but also give rise to some of the signs and symptoms associated with these disorders [16–18].

In the current study, the approach was to develop multifunctional drugs which would halt the apoptotic neuronal breakdown process and eliminate some of the signs and symptoms of diseases such as AD and PD by: (a) Inhibiting NMDA receptors and blocking *L*-type voltage gated calcium channels (VGCC) thus regulating the Ca^{2+} influx mediated excitotoxic process; (b) Inhibiting the MAO-B enzyme thus allowing increase in dopamine levels in the CNS and reducing the levels of the highly oxidative products produced by the activity of this enzyme; (c) Possess anti-apoptotic activity to halt the natural neuronal cell death process. With this in mind, we focused on the structures of pentacycloundecane (**1**), amantadine (**2**), rasagiline (**6**) and selegiline (**7**, Fig. 1).

Rasagiline and selegiline are second generation propargylamine derivatives that irreversibly inhibit brain MAO-B, and have promising neuroprotective activities [19]. After several years of study and research, it has been established that the neuroprotective effects of rasagiline and selegiline can be attributed to its propargyl moiety [16–18]. This observation was made on the grounds that propargylamine (**8**), itself exerts the same neuroprotective effects as offered by rasagiline. It has also been established that the MAO-B inhibiting activity is not a prerequisite for the neuroprotection provided by rasagiline, selegiline and propargylamine as these compounds have been shown to inhibit apoptosis through other anti-apoptotic mechanisms that may contribute to their possible disease-modifying activities [20,21]. Since MAO-B activity is increased in both AD and PD, MAO-B inhibitors may be of further therapeutic benefit [22].

Polycyclic cage compounds, such as pentacyloundecane (PCU, **1**), amantadine (**2**) and NGP1-01 (**3**) have various biological applications, with special interest in the symptomatic and proposed curative treatment of neurodegenerative diseases [23]. These compounds can be used to modify and improve the pharmacokinetic and pharmacodynamic properties of drugs and it is apparent from literature that the polycyclic cage is useful as both a scaffold for side-chain attachment as well as for improving a drug's lipophilicity [23]. This lipophilicity enhances a drug's transport across cellular membranes, including the selectively permeable blood–brain barrier, and increases its affinity for lipophilic regions in target proteins [23,24]. In addition, these polycyclic moieties afford metabolic stability, thereby prolonging the pharmacological effect of a drug, leading to a reduction of dosing frequency and improving patient compliance thereof [25]. The known NMDA receptor channel antagonism of these cage compounds, combined with their *L*-type calcium channel blocking activity, suggest that these polycyclic cage moieties may potentially serve as therapeutic agents for neurodegenerative disorders [10,23,26–28].

With the focus being on the development of multifunctional drugs, it was thus a rational decision to incorporate polycyclic cage moieties and propargylamine functional groups or derivatives thereof into the structures of the novel compounds to be synthesised, thus giving rise to a series of compounds with the inherent therapeutic profiles of the contributing moieties (i.e. NMDA receptor channel antagonism, *L*-type calcium channel blocking activity, MAO-B inhibitory activity and anti-apoptotic activity). A single compound exhibiting such an array of multifunctional neuroprotective activities may curb the neurodegenerative process more effectively than a compound which functions on only one of the many drug target sites available.

2. Results and discussion

2.1. Synthesis

In synthesising the novel polycyclic compounds (**9**–**16**, Fig. 2), propargylamine, propargylbromide or ethynyl magnesium bromide was reacted with the PCU (**1**, Cookson's diketone) or amantadine (**2**) scaffold to give the final compounds (Fig. 2). Each compound was synthesised to evaluate the activity and benefit of the presence of a certain group of atoms in the molecule. These groups included the following: a terminal acetylene group (**9**), an acetylene group between two non-polar groups (**10**), a secondary propargylamine connected to an oxa-PCU structure (**11**, **12**), a tertiary propargylamine conjugated to an aza-PCU structure (**13**, **14**) and an adamantane structure (**15**, **16**).

Starting from the PCU diketone (**1**) or the methyl-diketone (**a**, Scheme 1), depending on the compound to be synthesised, the reaction proceeded by conjugation of propargylamine through reductive amination with sodium borohydride, following steps i-iv to give the oxa-derivatives, **11** and **12**. The aza derivatives, **13** and **14**, were synthesised utilising sodium cyanoborohydride as reducing agent. Compound **9** was synthesised *via* the Grignard reaction through conjugation of ethynyl magnesium bromide with the methyl-diketone producing the title compound **9** (Scheme 1).

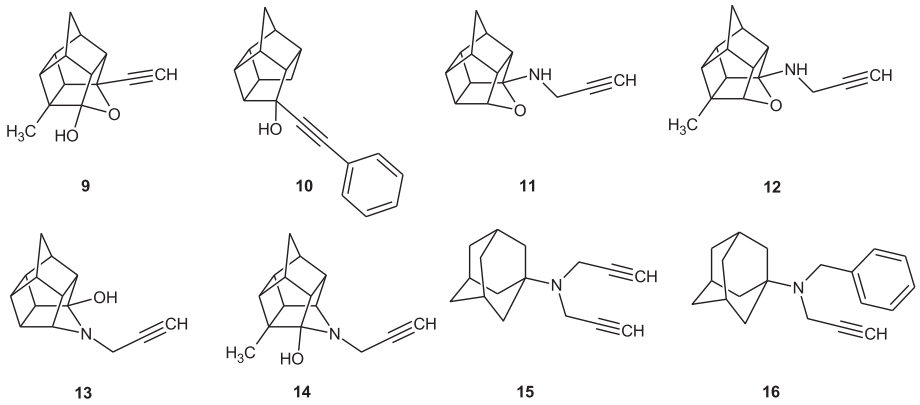

Fig. 2. Synthesised acetylene (**9** and **10**) and propagylamine (**11**–**16**) polycyclic compounds evaluated for anti-apoptotic activity, calcium modulating effects and MAO-B inhibition.

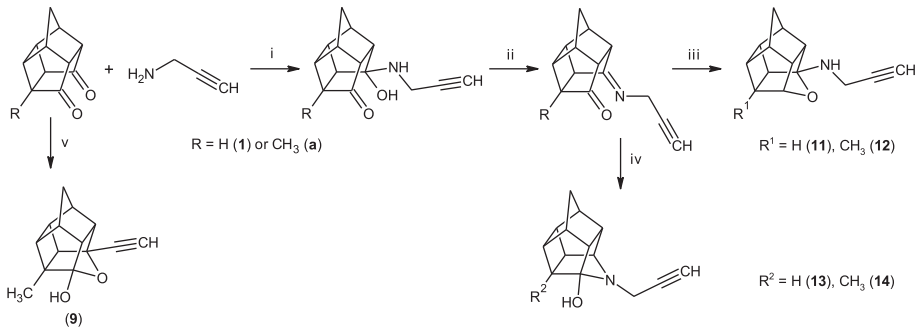

Scheme 1. Reagents and conditions: (i) THF, −10 °C, 45 min; ii) benzene, Dean–Stark, reflux, 1 h; (iii) THF/MeOH, $NaBH_4$, rt, 24 h; **11**, 10%; **12**, 27% (iv) THF/MeOH, $NaCNBH_4$, rt, 24 h; **13**, 16%; **14**, 4%; (v) THF, ethynyl magnesium bromide, rt, 21 h, **9**, 16%.

The synthesis of compound **10** commenced with the Cookson's diketone (Scheme 2), which was mono-protected as the corresponding ethylene acetal. The remaining ketone was reduced with lithium aluminium hydride and subsequent hydrolysis furnished the hydroxyl-ketone. Wolff-Kisher reduction of the hydroxyl-ketone under Huang-Minlon conditions gave the mono-alcohol, followed by oxidation with chromium trioxide to yield the mono-ketone (**b**). The mono-ketone (**b**) was conjugated to phenyl-acetylene in the presence of a potassium fluoride and alumina solution to yield the title compound **10** (Scheme 2).

The synthesis of compound **15** commenced through the conjugation of the primary amine of amantadine (**2**) and benzaldehyde with subsequent reduction, utilising LiAlH to give *N*-benzyl-adamantan-1-amine (**c**, Scheme 3). Propargylbromide was conjugated to (**c**), *via* a nucleophilic S_N2 substitution reaction, to produce compound **15**. Compound **16** was synthesised by means of microwave irradiation in the presence of an excess amount of propargylbromide (Scheme 3).

The PCU structures, compounds (**9**–**14**), were obtained and evaluated as racemic mixtures and the structure and geometry of representative compounds were recently confirmed using single X-ray crystallography and standard spectroscopy techniques [29].

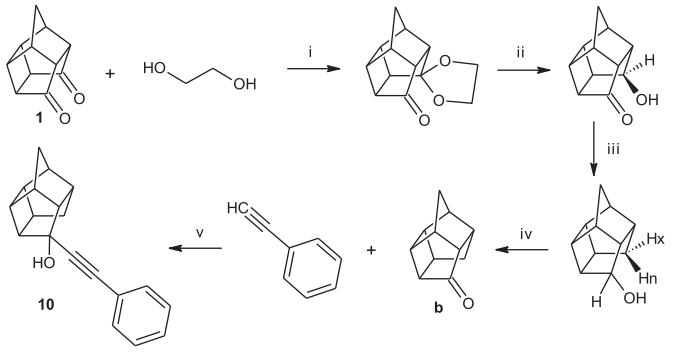

Scheme 2. Reagents and conditions: (i) *p*-TsOH (cat), benzene, Dean–Stark, reflux, 3.5 h, 95% (ii) $LiAlH_4$, Et_2O, reflux, 2 h then 6% aq HCl, rt, 2 h, 61%; (iii) $NH_2.NH_2.H_2O$, diethylene glycol, 120 °C, 1.5 h, then KOH, 190 °C, 3 h, 33%; (iv) CrO_3, H_2O, 94% aq CH_3COOH, 90 °C, 4 h, **b**, 84%; (v) KF/alumina, 60 °C, 12 h, **10**, 73%.

2.2. Anti-apoptotic activity

The compounds' anti-apoptotic activity were evaluated *in vitro* using the DePsipher™ kit, which marks changes in the mitochondrial membrane potential that takes place during apoptosis [30]. The quantitative and qualitative detection of apoptosis were done by means of flow cytometry, which made it possible to determine the percentage of cells that were still viable in the samples after treatment with the synthesised compounds. For this purpose SK-NBE(2) neuroblastoma cells were used, and apoptosis was induced using a serum-deprivation model. Control experiment 1 was included to evaluate the viability status of the cells, in the absence of test compound, with 1.25% dimethyl sulphoxide (DMSO, Fig. 3). The viability data was used to compare the data generated with the test compounds in order to determine if the test compounds attenuated the progression of the apoptotic process. With this control experiment the effect of 1.25% DMSO was also evaluated. Control experiment 2 was used to evaluate the viability of the cells and the progression of the apoptotic process in the absence of DMSO. When comparing the values of control experiments 1 and 2,

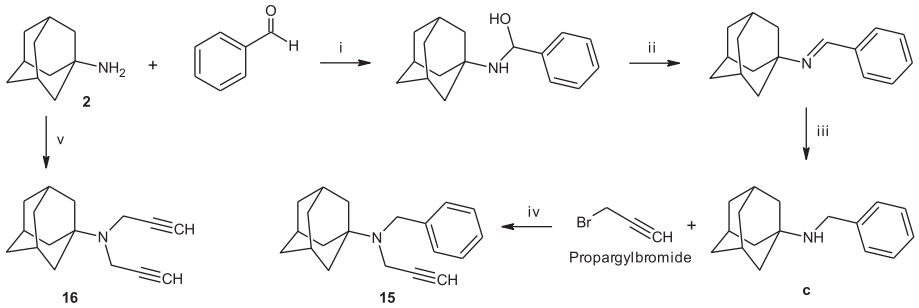

Scheme 3. Reagents and conditions: (i) EtOH, rt, 4 days, 59%; (ii) $-H_2O$; (iii) $NaBH_4$, reflux, 12 h, **c**, 59%; (iv) DMF, rt, 24 h; **15**, 25%; (v) Excess propargylbromide, aq NaOH, microwave (25 min, 80 °C–100 °C, 250 W); **16**, 91%.

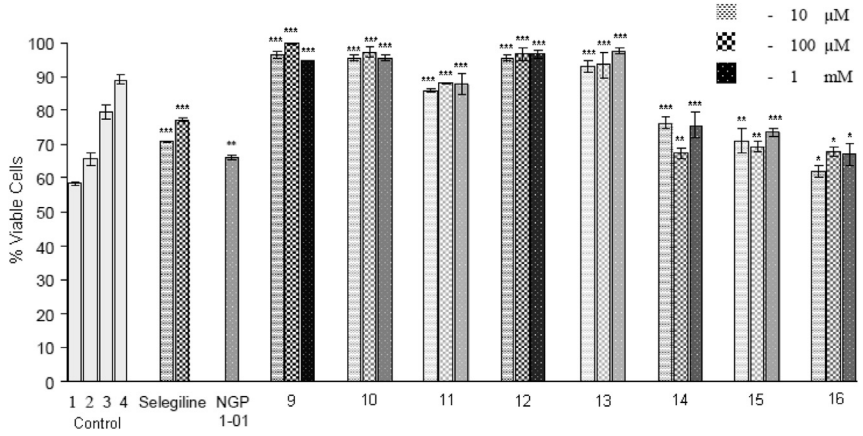

Fig. 3. Anti-apoptotic activity of the test compounds (*$p < 0.05$; **$p < 0.01$; ***$p < 0.001$).

it is clear that even though the final DMSO concentration in the samples was only 1.25%, it had a negative effect on the viability of the cells. In control experiment 2, which did not contain any DMSO, cell viability increased with 7.19%. It can thus be argued that the serum deprivation was not the only factor inducing apoptosis, but also the DMSO, which served as co-solvent for the test compounds. Control experiment 3 was used to evaluate the influence of re-introduction of serum rich medium, which significantly attenuated the apoptotic process. This control experiment was used to estimate the potencies of the test compounds as anti-apoptotic agents. Control experiment 4 was included to analyse and determine the viability status of the cells, when no apoptosis had been induced, and conditions had been favourable to the end of the experiment. It was also included to ensure that the cells analysed were indeed healthy before inducing apoptosis (see Section 4.3.1. for a complete explanation of the experimental procedure).

The novel compounds were all tested in triplicate at three different concentrations (1 mM, 100 μM and 10 μM). The positive control, selegiline, was evaluated in triplicate at two concentrations (100 μM and 10 μM, Fig. 3). Included in the assay was the prototype polycyclic cage moiety, 8-benzylamino-8,11-oxapentacyclo [5.4.$0^{2,6}$.$0^{3,10}$.$0^{5,9}$]undecane (NGP1-01) [31], which was also evaluated in triplicate at the highest concentration (1 mM). NGP1-01 is a well-known NMDA receptor channel inhibitor and calcium channel antagonist, and was evaluated for anti-apoptotic activity, as an abnormal increase in calcium levels can act as a trigger for apoptosis [10]. The positive control, selegiline, had 12–19% more cells that were healthy and wherein apoptosis had either not been induced or reached the level of mitochondrial depolarisation, compared to control experiment 1 (Fig. 3). When compared to control experiment 1, compounds **9**–**16** and NGP1-01 (**3**) all had significant anti-apoptotic activity improving cell health between 9% and 41%. The anti-apoptotic activity of **9**–**15** were the most significant ($p < 0.001$; Fig. 3). The compound with the highest anti-apoptotic activity was **9**, where all cultures treated exhibited only 0.5% apoptotic cells in the analysed samples. Compound **10** was slightly less active than compound **9**, with only 2.8% of the cells showing apoptosis (Fig. 3). Studying the results of these experiments, it is clear that the anti-apoptotic activity of propargylamine can most probably be attributed to the acetylene group, as compounds **9** and **10** have equivalent or even higher activity than compounds **11**–**16**. For activity, this acetylene group can either be terminal (**9**) or between two non-polar groups (**10**), with the terminal acetylene group having slightly higher activity. It was also confirmed that when linked to a polycyclic cage structure, propargylamine and acetylene derivatives displayed increased anti-apoptotic activity. Further investigation must be conducted to ascertain whether this reported activity is solely due to the acetylene group, the cage moiety, or the acetylene group in conjunction with a nearby electronegative atom/group.

Comparing the activity of compounds **11** and **13**, it seems that the tertiary propargylamine had slightly higher activity than the secondary propargylamine, but the oxa- and aza-compounds in general had comparable activity activities. In the case of the oxa-compounds (**11**, **12**), the methylated cage showed increased activity. With the aza compounds (**13**, **14**), this was not observed. The adamantane compounds (**15**, **16**) had significantly lower activities than that of the pentacycloundecane compounds **9**–**13**. Solubility problems were also experienced with compounds **15** and **16** at higher concentrations, which may contribute to the observed lower

anti-apoptotic action. It could also be attributed to the possibility that the pentacycloundecanes may have an increased ability to cross cell membranes due to their high degree of lipophilicity [23], which would result in increased intracellular concentrations of the compounds. Comparing the percentage healthy cells of the samples treated with test compounds **9**, **10**, **12** and **13**, with that of the control experiment 4, which is representative of healthy cells in a favourable environment, it is interesting to note that these samples had more healthy cells than that of control experiment 4. This may be attributed to the compounds inhibiting even baseline apoptotic processes.

Although NGP1-01 exhibited significant anti-apoptotic activity, the activities of the synthesised compounds (**9**–**16**) were shown to be higher in comparison. This might be due to NGP1-01 only inhibiting one of the triggers of apoptosis, namely excitotoxicity due to calcium flux into the neuronal cells, whereas the newly synthesised compounds possibly inhibit the apoptotic cascade, directly or indirectly, at more than one point. However, further evaluations of these compounds are necessary to ascertain this.

2.3. VGCC and NMDA receptor channel activity

All polycyclic propargylamine and acetylene derivatives (**9**–**16**) were screened at 100 μM for their potential inhibitory activity on VGCC and/or NMDA receptor (NMDAR) channel. They were assessed using the fluorescent ratiometric indicator, Mag-Fura-2/AM, and a fluorescent plate reader. KCl mediated calcium influx in murine synaptoneurosomes was used to evaluate the influence of the test compounds on the calcium influx *via* VGCC. NMDA/Glycine mediated calcium influx was used to evaluate the influence of the test compounds on calcium influx *via* the NMDA receptor channel. Both assays were carried out with reference to standard controls. Results are shown in Table 1.

Fresh synaptoneurosomes were prepared [32] from rat brain homogenate and incubated with the ratiometric fluorescent calcium indicator, Fura-2/AM. The synthesized compounds were incubated for 30 min and a 140 mM KCl or a 100 μM NMDA/Glycine solution, in the VGCC and NMDA assay respectively, was added to depolarize the cell membranes or to stimulate calcium flux through the respective channels. Calcium influx was then monitored based on the fluorescence intensity relative to that of a negative control (without inhibiting compound) over a 5 min period. Two positive controls were included in the VGCC assay; nimodipine, a commercially available dihydropyridine *L*-type calcium channel blocker and the prototype pentacycloundecane compound NGP1-01. Two positive controls were also included in the NMDAR assay; MK-801, a commercially available potent high affinity NMDAR channel blocker and NGP1-01.

The results obtained showed variable activities from the compound series (Table 1). Compound **16**, an adamantane derivative, showed the best VGCC inhibitory activity within this series (45%). This adamantine derived propargylamine compound showed activity higher compared to that of NGP1-01 (**7**, 27%). Although structurally similar to **16**, the substitution of the aromatic moiety of **16** with a propargyl moiety to give the di-substituted propargylamine adamantane compound (**15**), lead to a significant decrease in VGCC activity (18%). This observation indicates the importance of including the benzylamine moiety within these structures for optimal VGCC activity. The exact mechanism in which these compounds interact with the VGCC for activity is thus far unexplored. The presence of the polycyclic cage moieties in the series of compounds and similarities to NGP1-01 and other polycyclic cage benzylamines, supports a mechanism earlier described for NGP1-01 as being frequency- and voltage- dependent open calcium channel blockers [33].

These compounds also exhibited of the highest NMDAR channel inhibitory activities within this test series (52% and 59% for **15** and **16** respectively). This high activity might be attributed to the inclusion of the adamantane moiety, which has known NMDAR inhibitory activity. Within the pentacycloundecane (PCU) test series, compounds **10** (19%), **12** (26%) and **13** (18%) showed moderate VGCC blocking effects when compared to that of NGP1-01 (27%). The remaining PCU derivatives showed low (**9** and **14**) to no VGCC activity (**11**). It is interesting that the inclusion of a methyl group to the structure of the inactive oxa-PCU compound **11** to give compound **12** improved the VGCC activity by 26%. However, this trend was not observed for the aza-PCU compounds **13** (11%) and **14** (18%). NMDAR channel inhibition was observed for PCU compounds **10** (23%) and **12** (38%), which showed improved inhibitory activity when compared to NGP1-01 (18%). Compound **12** showed dual action on both VGCC (26%) and NMDAR (38%). This finding suggests that the inclusion of the methyl substituent contributes towards binding and activity on both these drug targets as the compound exhibited activity comparable to, and better than NGP1-01 on both the VGCC and NMDAR. Comparing the activities obtained with compound **12** to that of compound **14** (VGCC − 11%, NMDAR − 11%), suggests that the oxa compounds have better VGCC and NMDAR inhibitory activity compared to aza compounds. Removal of the methyl substituent from **14** to give compound **13** increased VGCC inhibitory activity to 18% but decreased NMDAR inhibitory action to only 4%. Compound **10**, which resembles NGP1-01 in the aromatic moiety, also showed dual action on the VGCC (19%) and NMDAR

Table 1
The biological activities of test compounds as indication of potential neuroprotective activity.

Compound	Molecular formula	Molecular weight (g/mol)	% Viable cells − apoptosis induced [10 μM]	% VGCC inhibition [100 μM]	% NMDA receptor inhibition [100 μM]	% MAO-B inhibition [300 μM]
Propagylamine	C_3H_5N	55.079	79***	n.d.	n.d.	19.93*
Selegiline	$C_{13}H_{17}N$	187.281	77***	n.d.	n.d.	93.33***
NGP1-01	$C_{18}H_{19}NO$	265.350	67**	27**	18*	14.57*
9	$C_{14}H_{14}O_2$	214.260	100***	10	Inactive	Inactive
10	$C_{19}H_{18}O$	262.346	98***	19	23	73.32***
11	$C_{14}H_{15}NO$	212.275	88***	Inactive	Inactive	Inactive
12	$C_{15}H_{17}NO$	226.302	97***	26	38***	11.67*
13	$C_{14}H_{15}NO$	213.275	93***	18*	4	5.83
14	$C_{15}H_{17}NO$	227.302	67***	11	11	10.83*
15	$C_{16}H_{21}N$	227.345	68***	18*	52***	14.00*
16	$C_{20}H_{25}N$	279.419	70***	45*	59*	20.13*
Nimodipine	$C_{21}H_{26}N_2O_7$	418.440	Inactive	100***	n.d.	n.d.
MK-801	$C_{16}H_{15}N$	221.297	n.d.	Inactive	100***	n.d.

Statistical analysis was performed on raw data, with asterisks indicating significant inhibitory effect [(*) $p < 0.05$, (**) $p < 0.001$, (***) $p < 0.0001$] when compared to the control. n.d. = not determined.

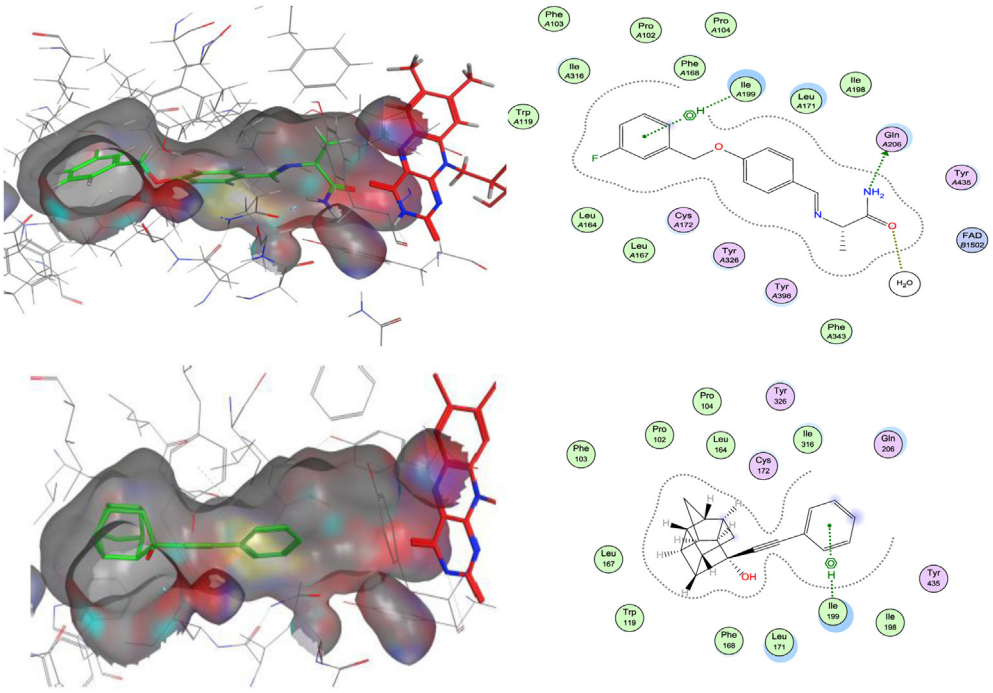

Fig. 4. Comparison between the putative binding modes of safinamide and compound **10** to the human MAO-B enzyme active site. The compounds and FAD cofactor in bold lines (online indicated in green and red respectively) with their respective binding interactions with the amino acid residues (sticks) shown on the right of each enzyme cavity representation. Safinamide and compound **10** show productive interactions with amino acid residues Ile-199 and Gln 205, and Ile-199, respectively.

(23%) as seen with NGP1-01, a known VGCC and NMDAR antagonist. It is suggested that these compounds (**9**–**16**) exhibit a blockade of the NMDA channel which is consistent with uncompetitive antagonism, similar to that reported for memantine. Memantine shares the phencyclidine (PCP)/tenocyclidine (TCP)/MK-801/ketamine binding site inside the NMDA channel pore. Radio-ligand binding studies with [3H]MK-801 and [3H]TCP, however, showed little or no displacement of PCU compounds, including NGP1-01, from this binding site. The functional block of calcium observed for the PCU structures needs to be further explored to elucidate the exact mechanism of action. We hypothesize that the series described in this paper will exhibit a similar mechanism of action and act as direct NMDA channel blockers [10].

2.4. MAO-B inhibitory activity

The synthesised compounds were also evaluated *in vitro* at various concentrations as inhibitors of MAO-B, using a spectrophotometric assay that utilised MMTP, an analogue of the neurotoxin MPTP as substrate, with baboon liver mitochondria serving as enzyme source. The potency of MAO-B inhibition was expressed as percentage inhibition of the MAO-B enzyme (Table 1). Only compound **10** showed significant MAO-B inhibition activity when compared to that of selegiline (93.22%), inhibiting the MAO-B enzyme by 73.32% at 300 μM. The rest of the compounds in the series either had no activity (**9**, **11**) or exhibited very limited inhibition, ranging from 5.83 to 20.13% (**12**–**16**). Comparing the MAO-B inhibition potencies of **11** with **12** and **13** with **14** reveals that in both cases the methyl group on the polycyclic cage, appeared to slightly increase MAO-B inhibition activity of the compounds. This may be ascribed to the enhanced interaction obtained with the non-polar entrance regions of the MAO-B enzyme.

For comparison, NGP1-01 was also evaluated as a MAO-B inhibitor, but no significant activity was observed. The compounds containing a phenyl side chain (**10**, **15** and selegiline), were consistently better inhibitors than the rest of the series and it can be speculated that these compounds were able to block the entrance cavity of the MAO-B enzyme active site (see Fig. 4). This may possibly be attributed to the planar character of the phenyl ring and possibly to the extended planar character of compound **10**. It has also been reported in literature that planar compounds frequently act as potent inhibitors of MAO-B [34,35]. Compound **10** contains both a hydroxyl and an extended planar phenyl moiety, which might further explain the significantly higher activity of **10** compared to that of the other synthesised compounds.

2.4.1. MAO-B molecular modelling

Computer-assisted simulated docking of compounds **9**–**16**, using Molecular Operating Environment (MOE), was carried out in an attempt to clarify the MAO-B inhibition activity – or lack thereof – for these structures [36]. The best-ranked docking solutions of the test compounds examined, showed that the proposed inhibitors occupy only the entrance cavity and barely access the substrate cavity of the MAO-B enzyme (PDB ID: 2V5Z, Fig. 4) [37]. In general, the amino acid residues between 120 and 220 are important in conferring substrate selectivity of MAO-B [38], most importantly residues Ile-199 (situated in the entrance cavity) and Gln-205 (situated in the substrate cavity). Interaction with these amino acid residues may confer a compound MAO-B inhibitory activity as shown by safinamide (Fig. 4), a known MAO-B inhibitor.

For compound **10** it was shown that the polycyclic moiety is stabilised within the entrance cavity with the extended planar phenyl moiety able to traverse deeper into the enzyme cavity and form the necessary interactions with Ile-199 (Fig. 4). This productive interaction between the phenyl function and the active site residue Ile-199 of the substrate cavity and/or the stabilisation of the polycyclic moiety to actively block the entrance cavity, might explain the MAO-B inhibitory activity observed for **10**. All the polycyclic moieties are stabilised within the hydrophobic entrance cavity and were unable to traverse deeper into the substrate cavity,

to from the necessary binding interactions with the flavin adenine dinucleotide (FAD) cofactor, which would have resulted in binding interactions and an increase the activity of these compounds (Fig. 4) [39,40]. Based on the molecular modelling results we are currently in process of developing a series of optimized PCU-propargylamine hybrid molecules with binding interactions and molecular orientations which might lead to enhanced MAO-B activity for these compounds. This series will enable the propargyl moiety to penetrate deeper into the cavity within close proximity of the FAD co-factor, similar to selegiline and rasagiline (data not shown) [19]. We also envision that the multifunctional activities shown for the current propargylamine derivatives will be retained in the new series.

3. Conclusion

This study aimed to develop compounds that would ultimately inhibit NMDA receptors, block VGCC and inhibit apoptotic processes as well as the MAO-B enzyme. Based on the results it can be concluded that compounds **10, 12, 15** and **16** showed the best range of activities. These compounds however showed little to no activity on the MAO-B enzyme except for 8-phenyl-ethynyl-8-hydroxy-pentacycloundecane (**10**) which inhibited the MAO-B enzyme by 73.32% at 300 μM. The compounds in the series all had significant anti-apoptotic activity comparable (**14**–**16**) to and better (**9**–**13**) than selegiline. Although the findings suggest compounds **9** and **11** to have little or no activity on the VGCC, NMDA receptors and MAO-B enzyme, the ability of these compounds to significantly inhibit apoptosis suggests that the compounds exhibit their neuroprotective action through some other mechanism(s) unexplored in this study. Having significant anti-apoptotic activity, this series of compounds might present interesting lead compounds in the design and development of more potent inhibitors. Further *in vitro* and *in vivo* studies into the anti-apoptotic cascade, dopamine transmission and blood–brain barrier permeability of these novel compounds are in process. Findings from these studies will elaborate on their potential as neuroprotective agents and might identify the point(s) at which these compounds inhibit the apoptotic process. The polycyclic propargylamines and acetylene derivatives thus have potential as novel multifunctional neuroprotective agents and further investigation is necessary to determine their maximum benefit in the treatment of neurodegenerative disorders.

4. Experimental

4.1. Chemistry: general procedures

Unless otherwise specified, materials were obtained from commercial suppliers and used without further purification. All reactions were monitored by thin-layer chromatography on 0.20 mm thick aluminium silica gel sheets (Alugram® SIL G/UV_{254}, Kieselgel 60, Macherey–Nagel, Düren, Germany). Visualisation was achieved using UV light (254 nm and 366 nm), an ethanol solution of ninhydrin or iodine vapours, with mobile phases prepared on a volume-to-volume basis. Chromatographic purifications were performed on silica gel (0.063–0.2 mm, Merck) except when otherwise stated. The mass spectra (MS) were recorded on an analytical VG 70-70E mass spectrometer using electron ionisation (EI) at 70 eV. Infra-red (IR) spectra were recorded on a Shimadzo IR prestige − 21 Fourier transform infrared spectrophotometer using KBr. Melting points were determined using a Gallenkamp and Stuart SMP-300 melting point apparatus and capillary tubes. All the melting points determined were recorded uncorrected. High resolution electron spray ionisation (HREI) mass spectra for all compounds were recorded on a Waters API Q-Tof Ultima mass spectrometer at 70 eV and 100 °C. All HREI samples were introduced by a heated probe and perfluorokerosene was used as reference standard. ^{1}H and ^{13}C NMR spectra were acquired on a Bruker Avance III 600 MHz spectrometer, with the ^{1}H spectra recorded at a frequency of 600.170 MHz and the ^{13}C spectra at 150.913 MHz. Tetramethylsilane (TMS) was used as internal standard, with $CDCl_3$ as solvent. All chemical shifts are reported in parts per million (ppm), relative to the internal standard. The following abbreviations are used to indicate the multiplicities of the respective signals: s − singlet; br s − broad singlet; d − doublet; dd − doublet of doublets; t − triplet; m − multiplet; and AB-q − AB quartet. The multiplicity of the identified carbons was confirmed with DEPT-spectra. Microwave synthesis was performed using a CEM Discover™ microwave synthesis system.

4.2. Synthesis of compounds

4.2.1. Pentacyclo[5.4.1.$0^{2,6}$.$0^{3,10}$.$0^{5,9}$]undecane-8-11-dione (***1***)

As described by Cookson et al. (1958, 1964) [41].

4.2.2. 1-Methyl-pentacyclo[5.4.1.$0^{2,6}$.$0^{3,10}$.$0^{5,9}$]undecane-8-11-dione (***a***)

As described by Marchand et al. (1984) [42].

4.2.3. Pentacyclo[5.4.1.$0^{2,6}$.$0^{3,10}$.$0^{5,9}$]undecane-8-one (***b***)

As described by Dekker and Oliver (1979) [43].

4.2.4. 8-Benzylamino-8,11-oxapentacyclo[5.4.$0^{2,6}$.$0^{3,10}$.$0^{5,9}$] undecane (NGP1-01, 3)

As described by Van der Schyf et al. (1986) [31].

4.2.5. 1-Methyl-8-ethynyl-11-hydroxy-8,11-oxapentacyclo [5.4.$0^{2,6}$.$0^{3,10}$.$0^{5,9}$]undecane (***9***)

A solution of 1-methyl-pentacyclo[5.4.1.$0^{2,6}$.$0^{3,10}$.$0^{5,9}$]undecane-8-11-dione (**a**) (1.88 g; 10 mmol) in dry tetrahydrofuran (10 mL) was added to an excess of ethynyl magnesium bromide (1.0 M solution in tetrahydrofuran) (2.838 mL; 22 mmol) under argon, whilst stirring. The resulting mixture was stirred at ambient temperature for 21 h. The reaction mixture was poured over saturated aqueous ammonium chloride (NH_4Cl) solution (100 mL), and the resulting suspension was extracted with diethyl ether (3 × 25 mL). The combined organic extracts were washed sequentially with water (25 mL) and brine (25 mL). The solvent was dried (Na_2SO_4) and filtered, and the filtrate was concentrated under reduced pressure. The residue, pale yellow oil, was successfully purified by precipitation from a mixture of ethyl acetate/petroleum ether (1:3), over a period of 24 h at ambient temperature. This yielded the pure product as a light brown powder (yield: 0.762 g; 3.170 mmol; 15.87%). **$C_{14}H_{14}O_2$**; **MW**, 214.3 g/mol; **mp**. 126 °C; **IR (KBr)** ν_{max}: 3260, 2125, 1211, 1031 cm^{-1}; **MS** (EI, 70 eV) *m/z*: 214 (M+), 186, 169, 158, 116, 91, 77, 39; **HR-ESI [M+H]$^+$**: calc. 215.1067, exp. 215.1069. **^{1}H NMR** (600 MHz, $CDCl_3$) δ_H: 3.72 (s, OH), 3.12–2.37 (m, 7H, H-2,3,5,6,7,9,10), 2.31 (s, 1H, H-13), 1.88:1.54 (AB-q, 2H, J = 10.4 Hz, H-4a,4b), 1.10 (s, 3H, CH_3); **^{13}C NMR** (150 MHz, $CDCl_3$) δ_C: 116.87 (1C, C-11), 81.18 (1C, C-8), 75.30 (1C, C-12), 61.84 (1C, C-13), 57.24 (1C, C-9), 56.91 (1C, C-7), 50.75 (1C), 47.46 (1C), 45.22 (1C), 43.49 (1C, C-4), 41.56 (1C), 39.19 (1C, C-1), 15.29 (1C, C-14).

4.2.6. 8-Phenylethynyl-8-hydroxy-pentacyclo[5.4.$0^{2,6}$.$0^{3,10}$.$0^{5,9}$] undecane (***10***)

Neutral alumina (60–80 mesh, 30 g) in water (150 mL) was added to a stirred solution of potassium fluoride (20 g) in water (150 mL). After 30 min the water was evaporated in a rotary evaporator at 80 °C. When most of the water had been removed, the remaining mixture was heated to, and maintained at 140–

150 °C under vacuum (5 mm Hg) overnight to afford 50 g of KF/alumina reagent. Phenylacetylene (255.350 mg; 2.500 mmol), pentacyclo[5.4.0^{2,6}.0^{3,10}.0^{5,9}]undecane-8-one (**b**, 480.650 mg; 3 mmol), and KF/alumina (2.500 g) were mixed in a 25 mL flask at 60 °C. The progress of the reaction was monitored by TLC. After 12 h the reaction mixture was washed with petroleum ether, filtered, and the solvent was evaporated under vacuum, affording a clear yellow oil. The residue was purified by means of column chromatography, by using a versa flash silica-gel column with petroleum ether/ethyl acetate (10:2) as eluent, to afford the product as a light yellow wax (yield: 480 mg; 1.830 mmol; 73.18%). **$C_{19}H_{18}O$; MW**, 262.4 g/mol; **mp.** 90 °C; **IR (KBr)** ν_{max}: 3069, 2225, 1599, 1491, 1125, 752 cm^{-1}; **MS** (EI, 70 eV) *m*/*z*: 262 (M+), 196, 183, 165, 129, 115, 91, 77; **HR-ESI [M+H]$^+$**: calc. 263.1430 exp. 263.1439; **^{1}H NMR** (600 MHz, $CDCl_3$) δ_H 7.36–7.13 (m, 5H, H 15,16,17,18,19), 2.77–2.28 (m, 8H, H-1,2,3,5,6,7,9,10), 1.93:1.60 (AB-q, 2H, H-11a,11b), 1.72:1.18 (AB-q, 2H, *J* = 10.4 Hz, H-4a,4b); **^{13}C NMR** (150 MHz, $CDCl_3$) δ_C: 131.51 (1C, C-14), 128.23 (2C, C-15,19), 128.10 (2C, C-16,18), 123.02 (1C, C-17), 94.15 (1C, C-8), 83.21 (1C, C-13), 75.91 (1C, C-12), 51.50 (1C), 47.27 (1C), 45.20 (1C), 44.95 (1C), 42.73 (1C, C-4), 41.50 (1C), 40.61 (1C), 36.62 (1C), 34.73 (1C), 28.98 (1C, C-11).

*4.2.7. 8-(N)-propargylamino-8,11-oxapentacyclo[5.4.0^{2,6}.0^{3,10}.0^{5,9}]undecane (**11**)*

Pentacyclo-[5.4.0^{2,6}.0^{3,10}.0^{5,9}]undecane-8-11-dione (**1**, 5 g; 0.029 mol) was dissolved in tetrahydrofuran (50 mL) and cooled to ± −10 °C, while stirring on an external bath, containing an acetone/NaCl/ice mixture. Propargylamine (1.600 g; 0.029 mol) was added drop-wise, with continued stirring of the reaction mixture at lowered temperature. The carbinolamine started precipitating after approximately 15 min, but the reaction was allowed to stir for an additional 30 min to reach completion. The carbinolamine was isolated by filtration and washed with ice cold THF. Water was removed azeotropically by refluxing the material in dry benzene (60 mL), under Dean–Stark dehydrating conditions for 1 h, or until no more water was collected in the trap. The benzene was removed under reduced pressure, which yielded the Schiff base as yellow oil. The Schiff base (imine) was then dissolved in a mixture of anhydrous methanol (30 mL) and anhydrous tetrahydrofuran (THF) (150 mL). Reduction was carried out by adding sodium borohydride ($NaBH_4$) (1.500 g; 0.040 mol) in excess, and stirring the mixture for 24 h at room temperature. The solvents were removed under reduced pressure, the residue suspended in water (100 mL) and extracted with methylene chloride (4 × 50 mL). The combined organic fractions were washed with water (2 × 100 mL), dried over anhydrous MgSO4 and evaporated under reduced pressure to yield a milky yellowish oil. Purification of the product mixture was accomplished using column chromatography on silica gel, with ethyl acetate/methylene chloride/petroleum ether (1:1:1) as eluent. This yielded the desired amine as a light yellow precipitate. Recrystallisation from absolute ethanol rendered the final product as a colourless microcrystalline solid (yield: 600 mg; 2.827 mmol; 9.75%). **$C_{14}H_{15}O_1N_1$; MW**, 213.28 g/mol; **mp.** 113 °C**; IR (KBr)** ν_{max}: 3306, 3238, 2124, 1485, 1153, 1000 cm^{-1}; **MS** (EI, 70 eV) *m*/*z*: 213 (M+), 184, 134, 118, 91, 77, 39; **HR-ESI [M+H]$^+$**: calc. 214.1226, exp. 214.1225. **^{1}H NMR** (600 MHz, $CDCl_3$) δ_H: 4.63 (t, 1H, *J* = 5 Hz, H-11), 3.57:3.56 (dd, 2H, *J* = 2.5 Hz, H-12a,12b), 2.80–2.39 (m, 8H, H-1,2,3,5,6,7,9,10), 2.26 (br s, NH), 2.21 (s, 1H, H-14), 1.88:1.52 (AB-q, 2H, *J* = 10.4 Hz, H-4a,4b); **^{13}C NMR** (150 MHz, $CDCl_3$) δ_C: 108.98 (1C, C-8), 82.81 (1C, C-11), 82.76 (1C, C-13), 70.92 (1C, C-14), 55.46 (1C, C-7/9), 54.76 (1C, C-7/9), 44.84 (1C), 44.65 (1C), 44.54 (1C), 43.3 (1C), 43.07 (1C, C-12), 42.04 (1C), 41.54 (1C), 33.07 (1C).

*4.2.8. 1-Methyl-8-(N)-propargylamino-8,11-oxapentacyclo[5.4.0^{2,6}.0^{3,10}.0^{5,9}]undecane (**12**)*

1-Methyl-penta-cyclo[5.4.0^{2,6}.0^{3,10}.0^{5,9}]undecane-8-11-dione (**a**, 5.460 g; 0.029 mol) was dissolved in tetrahydrofuran (50 mL) and cooled to ±10 °C, while stirring on an external bath containing an acetone/NaCl/ice mixture. Propargylamine (1.600 g; 0.029 mol) was slowly added with continued stirring of the reaction mixture at lowered temperature. The reaction mixture was stirred for an additional 1½ hours to reach completion. The THF was removed under reduced pressure, affording the carbinolamine as a red/brown oil. Water was removed azeotropically by refluxing this material in dry benzene (60 mL), under Dean–Stark dehydrating conditions for 1 h, or until no more water was collected in the trap. The benzene was removed under reduced pressure, which yielded the Schiff base as a brown oil. The Schiff base (imine) was dissolved in a mixture of anhydrous methanol (30 mL) and anhydrous tetrahydrofuran (150 mL). Reduction was carried out by adding sodium borohydride (1.500 g; 0.040 mol) in excess and stirring the mixture for 24 h at room temperature. The solvents were removed under reduced pressure, the residue suspended in water (100 mL) and extracted with methylene chloride (4 × 50 mL). The combined organic fractions were washed with water (2 × 100 mL), dried over anhydrous $MgSO_4$ and evaporated under reduced pressure to yield a milky dark brown oil. Purification of the product mixture was accomplished using column chromatography, with ethyl acetate/methylene chloride/petroleum ether (1:1:1) as eluent, yielding the desired amine as a dark brown oil (Yield: 1.753 g; 7.746 mmol; 26.71%). **$C_{15}H_{17}O_1N_1$; MW,** 227.3 g/mol; **IR (KBr)** ν_{max}: 3310, 3250, 2100, 1452, 1153, 1007 cm^{-1}; **MS** (EI, 70 eV) *m*/*z*: 227 (M+), 212, 198, 184, 158, 145, 131, 91, 77, 39; **HR-ESI [M+H]$^+$**: calc. 228.1383, exp. 228.1395. **^{1}H NMR** (600 MHz, $CDCl_3$) δ_H: 4.08 (d, 1H, *J* = 4.4 Hz, H-11), 3.57 (m, 2H, H-12a,12b), 2.73–2.20 (m, 7H, H- 2,3,5,6,7,9,10), 2.14 (br s, NH), 2.06 (d, 1H, *J* = 5.28 Hz, H-14), 1.86:1.51 (AB-q, 2H, *J* = 10.4 Hz, H-4a,4b), 1.15 (s, 3H, CH_3); **^{13}C NMR** (150 MHz, $CDCl_3$) δ_C: 109.73 (1C, C-8), 87.15 (1C, C-11), 82.65 (1C, C-13), 70.95 (1C, C-14), 54.97 (1C, C-9), 54.66 (1C, C-7), 50.74 (1C), 46.99 (1C), 43.58 (1C), 43.18 (1C), 38.91 (1C, C-1), 33.07 (1C, C-12), 19.85 (1C, C-15).

*4.2.9. 8-Hydroxy-(N)-propargyl-8,11-azapentacyclo[5.4.0^{2,6}.0^{3,10}.0^{5,9}]undecane (**13**)*

Pentacyclo-[5.4.0^{2,6}.0^{3,10}.0^{5,9}]undecane-8-11-dione (**1**, 5 g; 0.029 mol) was dissolved in tetrahydrofuran (50 mL) and cooled to ± −10 °C, while stirring on an external bath, containing an acetone/NaCl/ice mixture. Propargylamine (1.600 g; 0.029 mol) was added slowly with continued stirring of the reaction mixture at lowered temperature. The carbinolamine started precipitating after approximately 60 min, but the reaction was stirred for an additional 45 min to reach completion. This carbinolamine was isolated by filtration. Water was removed azeotropically by refluxing this material in dry benzene (60 mL), under Dean–Stark dehydrating conditions for 1 h, or until no more water was collected in the trap. The benzene was removed under reduced pressure and the Schiff base was used without further purification. It was dissolved in a solution of acetic acid (15 mL) and dry methanol (250 mL). To the resulting solution was added sodium cyanoborohydride ($NaBH_3CN$) (2.510 g; 40 mmol) portion wise, with stirring at room temperature over a period of 5 min. The resulting mixture was stirred at room temperature for 2 h. The reaction mixture was then concentrated under reduced pressure, and water (100 mL) was added to the residue. The resulting suspension was stirred and solid sodium bicarbonate was added portion wise until evolution of carbon dioxide ceased. Excess solid sodium bicarbonate (2.000 g) was added, and the aqueous suspension was extracted with methylene chloride (4 × 50 mL). The combined extracts were washed with water

(2 × 100 mL), dried with anhydrous magnesium sulphate and filtered. The filtrate was concentrated under reduced pressure. A yellow solid was thereby obtained. Purification of the product mixture was accomplished using column chromatography on silica, with ethyl acetate/methylene chloride/ethanol (10:5:1) as eluent. The desired amine was obtained as an off-white powder. Recrystallisation from cyclohexane rendered the final product as an off white microcrystalline solid (Yield: 960 mg; 4.501 mmol; 15.52%). **$C_{14}H_{15}O_1N_1$; MW,** 213.3 g/mol; **mp.** 140 °C; **IR (KBr)** ν_{max}: 3225, 3100, 2114, 1120, 1070, cm^{-1}; **MS** (EI, 70 eV) *m/z*: 213 (M+), 196, 174, 147, 134, 118, 91, 77, 39; **HR-ESI [M+H]$^+$**: calc. 214.1226, exp. 214.1222; **^{1}H NMR** (600 MHz, $CDCl_3$) δ_H: 3.71 (s, 1H, H-12), 3.35 (d, 1H, J = 16.5 Hz, H-11), 3.00–2.43 (m, 8H, H-1,2,3,5,6,7,9,10), 2.25 (s, 1H, H-14), 1.82:1.49 (AB-q, 2H, J = 10.4 Hz, H-4a,4b); **^{13}C NMR** (150 MHz, $CDCl_3$) δ_C: 125.53 (1C, C-8), 81.23 (1C, C-13), 71.37 (1C, C-14), 65.52 (1C, C-11), 45.62 (1C, C-7/9), 43.12 (1C, C-7/9), 41.74 (1C, C-4), 41.60 (1C), 36.79 (1C), 30.33 (1C, C-12).

4.2.10. 1-Methyl-8-Hydroxy-(N)-propargyl-8,11-azapentacyclo [5.4.$0^{2,6}$.$0^{3,10}$.$0^{5,9}$]undecane (**14**)

1-Methyl-pentacyclo[5.4.$0^{2,6}$.$0^{3,10}$.$0^{5,9}$]undecane-8-11-dione (**b**, 10.658 g; 56.620 mmol) was dissolved in tetrahydrofuran (50 mL) and cooled to ± −10 °C, while stirring on an external bath containing an acetone/NaCl/ice mixture. Propargylamine (3.119 g; 56.620 mmol) was added drop wise with continued stirring of the reaction mixture at lowered temperature. The reaction mixture was stirred for 5½ hours to reach completion. The THF was removed under reduced pressure, affording a red/brown oil, the carbinolamine. Water was removed azeotropically by refluxing this material in dry benzene (60 mL), under Dean–Stark dehydrating conditions for 1 h, or until no more water was collected in the trap. The benzene was removed under reduced pressure, which yielded the Schiff base as a dark brown oil. The Schiff base was used without further purification. It was dissolved in a solution of acetic acid (30 mL) in dry methanol (500 mL). To the resulting solution, sodium cyanoborohydride (3.970 g; 63 mmol) was added portion wise, with stirring at room temperature over a period of 5 min. The resulting mixture was stirred at room temperature for 14 h. The reaction mixture was then concentrated under reduced pressure, and water (150 mL) was added to the residue. The resulting suspension was stirred, and solid sodium bicarbonate was added portion wise until evolution of carbon dioxide ceased. Excess solid sodium bicarbonate (3.000 g) was added, and the aqueous suspension was extracted with methylene chloride (4 × 50 mL). The combined extracts were washed with water (2 × 100 mL), dried with anhydrous magnesium sulphate, and filtered. The filtrate was concentrated under reduced pressure, leaving a deep orange oil as residue. Purification of the product mixture was accomplished using column chromatography on silica, with ethyl acetate/tetrahydrofuran (5:1) as eluent. This yielded the desired amine as a light yellow oil, which precipitated when ethanol was added. Recrystallisation from ethanol rendered the final product as a light yellow microcrystalline solid (Yield: 555 mg; 2.442 mmol; 4.31%). **$C_{15}H_{17}O_1N_1$; MW**, 227.3 g/mol; **mp.** 125 °C; **IR (KBr)** ν_{max}: 3225, 3078, 2124, 1119, 1070 cm^{-1}; **MS** (EI, 70 eV) *m/z*: 227 (M+), 188, 134, 118, 91, 77, 39; **HR-ESI [M+H]$^+$**: calc. 228.1388, exp. 228.1392; **^{1}H NMR** (600 MHz, $CDCl_3$) δ_H: 3.46–3.34 (m, 1H, H-11), 3.22:3.09 (d, 2H, J = 17.3 Hz, H-12a,12b), 2.57–2.09 (m, 8H, H-2,3,5,6,7,9,10,14), 1.60:1.06 (AB-q, 2H, J = 10.4 Hz, H-4a,4b), 1.19 (s, 3H, CH_3); **^{13}C NMR** (150 MHz, $CDCl_3$) δ_C: 125.53 (1C, C-8), 80.31 (1C, C-13), 72.68 (1C, C-14), 57.40 (1C, C-11), 46.62 (1C, C-9), 46.10 (1C, C-7), 45.09 (1C), 41.54 (1C, C-4), 37.63 (1C), 36.33 (1C), 34.52 (1C), 30.32 (1C, C-12), 21.98 (1C, C-15).

4.2.11. N,N-Dipropargyl-adamantan-1-amine (**15**)

Excess propargylbromide (0.595 mL; 6.677 mmol), amantadine (**2**, 302.49 mg; 2 mmol) and aqueous sodium hydroxide (NaOH) solution (180 mg in 6 mL water; 4.5 mmol) were placed in a round-bottom glass flask equipped with a condenser and a magnetic stirrer. The flask was placed in a CEM discover focused microwave synthesis system, and subjected to microwave irradiation at 80–100 °C (power 250 Watt) for 25 min. After completion of the reaction, the product was extracted into ethyl acetate. The solvent was then removed under reduced pressure. The unreacted amantadine was removed from the residue by adding acetone to the residue and collecting the amantadine by filtration. The acetone was then removed under reduced pressure from the filtrate, affording orange crystals which were recrystallised out of ethyl acetate to afford the pure product as light yellow crystals (412 mg; 1.812 mmol; 90.61%). **$C_{16}H_{21}N_1$; MW**, 227.35 g/mol; **mp.** 76 °C; **IR (KBr)** ν_{max}: 3237, 2099, 1119 cm^{-1}; **MS** (EI, 70 eV) *m/z*: 227 (M+), 184, 144, 132, 91, 79, 53, 39; **HR-ESI [M+H]$^+$**: calc. 228.1752, exp. 228.1755; **^{1}H NMR** (600 MHz, $CDCl_3$) δ_H: 3.65 (s, 4H, H 11a,11b,14a,14b), 2.17 (s, 2H, H-13,16), 2.06 (s, 3H, H-3,5,8), 1.80 (s, 6H, H-2a,2b,6a,6b,7a,7b), 1.63–1.46 (m, 6H, H-4a,4b,9a,9b,10a,10b); **^{13}C NMR** (150 MHz, $CDCl_3$) δ_C: 82.12 (2C, C-12,15), 72.08 (2C, C-13,16), 55.45 (1C, C-1), 39.96 (3C, C-3,5,8), 36.54 (3C, C-2,6,7), 35.03 (2C, C- 11,14), 29.70 (3C, C-4,9,10).

4.2.12. N-Propargyl-N-benzyl-adamantan-1-amine (**16**)

A solution of amantadine (**2**, 5 g; 33.056 mmol) and benzaldehyde (3.51 g; 33.073 mmol) in ethanol (60 mL) was stirred for 4 days at ambient temperature under nitrogen atmosphere. The solvents were removed *in vacuo*. The resulting oil was dissolved in 80 mL benzene and refluxed under Dean–Stark conditions for 6 h, where after the benzene was removed *in vacou*. The resulting reaction mixture was dissolved in 60 mL ethanol and solid sodium borohydride ($NaBH_4$) (2.5 g; 66.085 mmol) was then added slowly in small portions over 30 min, and stirring of the resulting suspension was continued at room temperature for 30 min under nitrogen atmosphere. The reaction mixture was refluxed for 12 h. After cooling to ambient temperature, the mixture was diluted with ethanol (60 mL), and the excess sodium borohydride was destroyed by adding aqueous hydrochloric acid (HCl) (10 mL, 5 M) drop wise. The reaction mixture was then made alkaline, to pH 12, by adding aqueous sodium hydroxide (NaOH) solution. Finally, the desired product was extracted to methylene chloride (4 × 10 mL) and dried over anhydrous magnesium sulphate ($MgSO_4$). The solvent was evaporated under reduced pressure to afford the intermediate product, *N*-benzyl-adamantan-1-amine (**c**), as white crystals (yield: 4.757 g; 19.6 mmol; 59.29%). This intermediate product was subsequently used in the following steps without any further purification. A solution was made of *N*-benzyl-adamantan-1-amine (**c**, 4.757 g; 19.6 mmol) and excess propargylbromide (2.3 mL; 25.81 mmol) in dry dimethylformamide (30 mL), and left for 24 h to react at ambient temperature. After this period of time the mixture was diluted with water (50 mL), and an extraction was done using methylene chloride (DCM) (3 × 50 mL) and dried over anhydrous sodium sulphate (Na_2SO_4). The solvent was removed under reduced pressure to afford a thick dark orange residue. The desired product was precipitated out of the residue by the addition of chloroform (30 mL), which allowed the collection of the final product by filtration as an off-white powder (yield: 1.352 g; 4.82 mmol; 24.59%). **$C_{20}H_{25}N_1$; MW,** 279.3 g/mol; **mp.** 81 °C; **IR (KBr)** ν_{max}: 3210, 3062, 2091, 1495, 1130, 748 cm^{-1}; **MS** (EI, 70 eV) *m/z*: 279 (M+), 236, 222, 185, 135, 91; **HR-ESI [M+H]$^+$**: calc. 280.2065, exp. 280.2063; **^{1}H NMR** (600 MHz, $CDCl_3$) δ_H: 7.35–7.20 (m, 5H, H- 16,17,18,19,20), 3.84 (s, 2H, H-14a,14b), 3.32 (s, 2H, H-11a,11b), 2.15 (s, 3H, H-3,5,8), 2.09 (s, 1H, H-13), 1.90 (s, 6H, H-

2a,2b,6a,6b,7a,7b), 1.65 (s, 6H, H-4a,4b,9a,9b,10a,10b); **^{13}C NMR** (150 MHz, $CDCl_3$) δ_C: 141.11 (1C, C-15), 128.65 (2C, C-16,20), 128.18 (2C, C-17,19), 126.66 (1C, C-18), 83.22 (1C, C 12), 72.08 (1C, C-13), 55.05 (1C, C-1), 48.98 (1C, C-14), 40.53 (3C, C-3,5,8), 36.77 (3C, C-2,6,7), 34.79 (1C, C-11), 29.86 (3C, C-4,9,10).

4.3. Biological evaluations

4.3.1. Apoptosis detection – DePsipher™ assay

DePsipher™ utilises a lipophilic cation (5,5′,6,6′-tetrachloro-1,1′,3,3′-tetraethylbenzimidazolyl carbocyaniniodide), which can be used as a mitochondrial activity marker to evaluate the viability of a cell population, detecting early apoptosis, and evaluating the effect of drugs on the cell population [30]. The cation aggregates upon membrane polarisation, forming an orange-red fluorescent compound. If the potential is disturbed, the dye cannot access the transmembrane space and remains orange-red or reverts to its green monomeric form. Thus, healthy cells present both the polymeric (orange-red) and monomeric (green) form of the cation, with the monomeric form residing in the cytoplasm and the aggregated form in the transmembrane space. It can be concluded that in comparison with healthy cells, wherein apoptosis has not been induced, the ratio of orange-red fluorescence to green fluorescence of apoptotic cells will be lower. The fluorescence can be observed and measured by flow cytometry with the red aggregates having absorption/emission maxima of 585/590 nm, and the green monomers absorption/emission maxima of 510/527 nm.

4.3.1.1. Biological material

4.3.1.1.1. Cell cultivation. In the current study the SK-N-BE(2) neuroblastoma cells were used to evaluate the anti-apoptotic activity of the synthesised compounds. The cells were cultivated in serum-rich growing medium, consisting of F12 nutrient (F12) supplemented with 10% foetal bovine serum (FBS), 1% penicillin/streptomycin (Pen/Strep) (10 000 units/100 mL stock) and 0.1% fungizone (FZ) (2.5 μg/mL units stock). They were incubated at 37 °C in a 5% CO_2 and 95% O_2 humidified atmosphere. The cells duplicated every 30–48 h and when a confluency of 80% was reached, the adherent cells were detached from the flask bottom by means of trypsination. To ensure complete detachment of the cells, they were incubated with trypsine for approximately 10 min. After trypsination, the cells were seeded in new flasks at a density of no less than 1/6 confluency.

4.3.1.1.2. Induction of apoptosis. In the current study, trophic factor deprivation/serum starvation was used to induce apoptosis in cells. With growth factors being essential to the normal development and survival of neuronal cells, a shortage thereof would cause neurons to compete with one another for neurotrophic factors, with the unsuccessful ones dying. With no serum (neurotrophic factors) available, all the cells will die in a given time. The serum deprived medium consisted of F12, Pen/Strep and FZ in the same ratio as mentioned in Section 4.3.2.2.

4.3.1.1.3. Cells used to evaluate anti-apoptotic activity of compounds. After the cells reached 80% confluency, the serum rich medium was replaced with serum deprived medium. The cells were then incubated under normal conditions (see Section 4.3.2.2) for a period of 24 h, which was sufficient time for apoptosis to be induced. Examining the cells under the microscope after this period of time, it was clear that their morphology had changed. The cells were no longer attached to the bottom of the flask, and their shape had also changed from the sprouting appearance to a spherical shape, being indicative of unhealthy cells. After being incubated in the serum deprived medium for the indicated time, the medium was removed, using centrifugation. The cells were then seeded in 24-well plates, with each well containing a concentration of 1 x 106 cells per 2 mL of serum deprived medium containing the test compounds, which were dissolved in dimethyl sulphoxide. Final concentrations of samples to be analysed contained 1.25% (v/v) DMSO. The cells were then incubated under normal conditions for a period of 36 h before being analysed. The test compounds (**6**–**13**) were all tested in triplicate at three different concentrations (1 mM, 100 μM and 10 μM). The positive control, selegiline, was tested in triplicate at two concentrations (100 μM and 10 μM). Included into the research was NGP1-01 which was also tested in triplicate at the highest concentration (1 mM).

4.3.1.1.4. Cells used for control experiments. In this study four control experiments were included.

4.3.1.1.4.1. Control experiment 1

After the cells reached 80% confluency, the serum rich medium was replaced with *serum deprived medium*. The cells were then incubated under normal conditions for a period of 24 h. After being incubated in the *serum deprived medium*, the medium was removed by centrifugation. The cells were subsequently seeded in 24-well plates, with each well containing a concentration of 1 x 106 cells per 2 mL of *serum deprived medium* and DMSO (1.25% (v/v)). After this, the cells were incubated under normal conditions (37 °C in a 5% CO_2 and 95% O_2 humidified atmosphere) for a period of 36 h before being analysed. Control experiment 1 was included to evaluate the viability status of the cells in the absence of test compound. The viability data will be compared to the data generated with the test compounds in order to determine if the test compounds attenuated the progression of the apoptotic process. With this control experiment, the effect of DMSO was also evaluated.

4.3.1.1.4.2. Control experiment 2

After the cells reached 80% confluency, the serum rich medium was replaced with *serum deprived medium*. The cells were then incubated under normal conditions for a period of 24 h. After being incubated in the *serum deprived medium*, the medium was removed by centrifugation. The cells were subsequently seeded in 24-well plates, with each well containing a concentration of 1 x 106 cells per 2 mL of *serum deprived medium* with no DMSO content. The cells were incubated under normal conditions for a period of 36 h before being analysed. Control experiment 2 was used to evaluate the effect of DMSO on the viability of the cells and on the progression of the apoptotic process.

4.3.1.1.4.3. Control experiment 3

After the cells reached 80% confluency, the serum rich medium was replaced with *serum deprived medium*. The cells were subsequently incubated under normal conditions for a period of 24 h. After being incubated in the *serum deprived medium*, the medium was removed by centrifugation. The cells were then seeded in 24-well plates, with each well containing a concentration of 1 x 106 cells per 2 mL of fresh *serum rich medium* with no DMSO present. After this the cells were incubated under normal conditions for a period of 36 h before being analysed. Since the re-introduction of serum rich medium is expected to significantly attenuate the apoptotic process, this control experiment will be used to estimate the potencies of the test compounds as anti-apoptotic agents.

4.3.1.1.4.4. Control experiment 4

After the cells reached 80% confluency, the serum rich medium was replaced with *fresh serum rich medium*. The cells were then incubated under normal conditions for a period of 24 h. After being incubated in the *serum rich medium*, the medium was removed by centrifugation. The cells were subsequently seeded in 24-well plates, with each well containing a concentration of 1 × 106 cells per 2 mL of *serum rich medium* with no DMSO present. The cells were incubated under normal conditions for a period of 36 h before being analysed. Control experiment 4 was included to analyse and determine the viability status of the cells, when no apoptosis had

been induced, and conditions had been favourable to the end. It was also included to ensure that the cells analysed were indeed healthy before inducing apoptosis.

4.3.1.2. Assay procedure. The cells of each sample were harvested consecutively as follows: After incubating the cells for 36 h, the medium was removed from the cells using centrifugation. The cells that had adhered to the bottom of the flasks were removed by trypsination. The trypsine/cell mixture was added to the cells from which the medium had been removed. The trypsine was removed from the cells by centrifugation at 500 × *g* for 5 min at room temperature. The cells of each sample were then resuspended in 1 mL of diluted DePsipher solution, consisting of 1 μL DePsipher dye and 1 mL of pre-warmed F12 medium. The cells were incubated for 20 min at 37 °C and 5% CO_2. The samples were washed twice in PBS, and centrifuged at 500 × *g* between each wash. The cells were subsequently resuspended in 1 mL PBS and immediately taken to be analysed on the flow cytometer. The samples were kept shielded from light until analysis, since the DePsipher™ agent is light sensitive.

4.3.1.3. Data analysis. Analysis of the samples were performed on a BD FacsCalibur® flow cytometer [Becton Dickinson, San Jose (USA)], equipped with a 15 mV 488 nm, air-cooled argon-ion laser. Cells were gated in a forward scatter/side scatter plot to exclude debris. Green and red fluorescence were detected in the corresponding FL-1 and FL-2 photomultipliers through 530 nm (FITC) or 585 nm (PE/PI) bandpass filters respectively. In generating the data, the flow cytometer was set to analyse 50 000 events/cells. Figs. 1–3 (Supplementary Material) contains representative pseudo-colour graphs of every sample, which was generated using FlowJo®, based on the data of the flow cytometry. On the *x*-axis the FL-1 (green) fluorescence intensity is plotted, and on the *y*-axis the FL-2 (red) fluorescence intensity is plotted. Both intensities are measured in MFI (mean fluorescence intensity). Each spot is representative of a single cell analysed with the flow cytometer. The graphs are divided into four separate quadrants, each containing a population of cells, which exhibit the same characteristics. In the upper left quadrant (Q1) lies all the cells which emit only red fluorescence, whereas the cells which emit only green fluorescence can be found in the lower right quadrant (Q4). The cells which emit both wavelengths of fluorescence can be found in the upper right quadrant (Q2), and the cells emitting neither of the two in the lower left quadrant (Q3). The following can be concluded by taking note of the explanations of the different quadrants as well as the characteristics of cells in each of these quadrants: As healthy cells contain both the monomeric and polymeric form of the cation dye, and would thus have intensity in both the FL1 and FL2 channels used to analyse the samples, the MFI values of these cells will lie in Q2 (see control experiment 4). The cells with MFI values in Q1 have only red fluorescence, which might be due to low concentrations of the dye inside the cell, indicating that all the monomers were polymerised. All these cells can thus also be said to be healthy, together with these found in Q2. Cells wherein apoptosis have been induced only contain the monomeric form of the dye, will not colour red at all, and will thus have MFI values in Q4. The cells lying in Q3 have not been dyed successfully or intensively enough, and have thus not coloured either red or green. From the pseudo-colour graphs it is clear that there was a difference in the number of apoptotic/healthy cells present in the different samples. Control experiment 1 had the least MFI values in Q1+Q2, and control experiment 4 the most. The MFI values of the other samples were either between the values of control experiments 1 and 4, or just above that of control experiment 4 (All pseudo-colour graphs are supplied in the Supplementary Material).

The data generated by these flow cytometry experiments were used to determine if the test compounds have anti-apoptotic properties on cultured cells. The values utilised to quantify cell viability were determined by the flow cytometer. Equation (1) was used to calculate the percentage of cells which were still viable in the samples analysed. In determining this value, the amount of cells in quadrant 1 (Q1), quadrant 2 (Q2) and quadrant 3 (Q3) and the total amount of events analysed (Qtotal) were utilised.

$$\%\ \text{Viable cells} = [(Q1 + Q2)/(Q\text{total} - Q3)] \times 100 \quad (1)$$

The results confirmed that a significant percentage of the cells had indeed coloured successfully with the dye. The percentage of the coloured cells that had fluorescence intensity in the FL2 channel, gave a quantitative indication of the number of healthy cells present in each sample, wherein apoptosis had not progressed or been induced. In control experiment 1, 41.62% of the cells were apoptotic, with only 58.38% remaining healthy. This indicates that the method of apoptosis induction had indeed been successful. Comparing the values of control experiments 1 and 2, it is clear that even though the final DMSO content in the samples was only 1.25%, it had a negative effect on the health of the cells. In control experiment 2, which did not contain any DMSO, there were 7.19% more cells that were healthy. It can thus be said that the serum deprivation was not the only factor inducing apoptosis, but also the DMSO which served as solvent for the test compounds.

4.3.2. NMDA and VGCC assays

4.3.2.1. Animals. The study protocol was approved by the Ethics Committee for Research on Experimental Animals of the University of the Western Cape (SRIRC 2012/06/13). Adult Winstar rats were sacrificed by decapitation and the brain tissue was removed and kept on ice for homogenation. After homogenation, the alliquoted brain homogenate was immediately used in the subsequent assay.

4.3.2.2. Methods. The fluorescent ratiometric indicator, Mag-Fura-2/AM, and a Bio-Tek® fluorescence plate reader were used to evaluate the influence of the test compounds on calcium homeostasis *via* the VGCC and NMDA receptor channels utilizing murine synaptoneurosomes. Preparation of synaptoneurosomes, solutions and experimental techniques were similar to those of published studies [26,44a–d]. All data analysis, calculation and graphs were done using Prism 6.0® (GraphPhad, La Jolla, CA). Data analysis was carried out using the Student Newman Keuls multiple range test and the level of significance was accepted at $p < 0.05$.

4.3.2.3. Preparation of synaptoneuromes. Adult Winstar rats were used. Rats were sacrificed by decapitation, and the whole brains were removed. Whole-brain synaptoneurosomes were prepared by the techniques of Hollingsworth et al. [45], modified slightly. The brain from one rat was homogenized (8 strokes by hand using a glass homogenizer) in 30 mL of ice-cold incubation buffer (NaCl, 118 mM; KCl, 4.7 mM; MgCl, 1.18 mM; $CaCl_2$ 0.1 mM; HEPES, 20 mM and glucose, 30.9 mM pH 7.4). From this step forward the homogenate was kept ice-cold at all times to minimize proteolysis throughout the isolation procedure. The tissue suspension was placed in a 50 mL polycarbonate tube and then centrifuged for 5 min at 1000 g and 0 °C using a Labofuge 20® centrifuge. After centrifugation, the supernatant was decanted into a 50 ml polycarbonate tube and placed on ice. The supernatant was then divided into 2 mL eppendorf vials whose weight had been previously recorded. This was followed by a second centrifugation at 15000 g for 20 min at 0 °C. The supernatant was discarded and the mass of the resulting pellet was calculated. Sufficient calcium-free buffer (NaCl, 118 mM; KCl, 4.7 mM; MgCl, 1.18 mM; HEPES, 20 mM

and glucose, 30.9 mM pH 7.4) was added to obtain a 3 mg/ml protein concentration (protein yield is approximately 10 mg/g of tissue) [45]

4.3.2.4. General procedure for loading FURA-2 AM and incubating test compounds. Experiments were carried out at 37 °C and fluorescence was measured with a flourescent plate reader (Bio-Tek®). 1990 μl of synaptoneurosome suspension prepared above was allowed to reach room temperature, thereafter 10 μl of Fura-2 AM (1 mM in DMSO) was added to produce a final concentration of 5 μM. Synaptoneurosomes were then incubated at 37 °C for 30 min after which the suspension was centrifuged on a desktop centrifuge at 7000 g for 5 min and the supernatant decanted to remove all extracellular Fura-2 AM. The resulting pellet was resuspended in 2 mM $CaCl_2$ containing buffer to obtain a final protein concentration of 0.6 mg/ml.

4.3.2.5. Measurement of intracellular calcium. For the screening test 10 mM stock solutions of the compounds in DMSO were prepared, with the control containing 1% DMSO and no test compound. 2 μl of the individual stock solutions were added to a 96 well plate in triplicate followed by the addition of 200 μl of synaptoneurosomal-Fura-2 AM solution prepared above. This gave rise to a final concentration of 100 μM of the compounds. The 96 well plate was shaken and incubated for 30 min at 37 °C and used immediately after incubation. The measurement was then performed at 37 °C in a 96 well plate using dual wavelength excitation at 340 nm and 380 nm. The resting fluorescence was measured at 510 nm after which the changes in fluorescence intensity following the addition of 10 μl depolarizing solution using auto-injectors was recorded over a period of 5 min. The changes in fluorescence indicated the effect of the test compound on calcium flux.

4.3.2.6. KCl mediated calcium stimulation. The wavelengths selected were 340 nm and 380 nm for excitation and 510 nm for emission, with a runtime of 5 min with 5 ms intervals. The test compound was incubated for 30 min at 37 °C and used immediately after incubation. The procedure was initiated and kept at 37 °C. At 10 s into the recording 10 μl of KCl (140 mM) depolarization solution (5.4 mM NaCl, 140 mM KCl, 10 mM $NaHCO_3$, 1.4 mM $CaCl_2$, 0.9 mM $MgSO_4$, 5.5 mM Glucose monohydrate, 0.6 mM KH_2PO_4, 0.6 mM Na_2HPO_4, and 20 mM HEPES. pH adjusted to 7.4 with NaOH) was added to the membrane preparation to depolarize the synaptoneurosomes and activate the calcium flux (addition was done using auto-injectors). Experiments were repeated three times on different tissue preparations with three determinations in each replicate.

4.3.2.7. NMDA/glycine mediated calcium stimulation. The wavelengths selected were 340 nm and 380 nm (excitation) and 510 nm (emission) with a runtime of 5 min with 5 ms intervals. The test compound was incubated for 30 min at 37 °C and used immediately after incubation. The procedure was initiated and kept at 37 °C. At 10 s into the recording 10 μl of NMDA/Glycine (0.1 mM) depolarization solution (0.1 mM $CaCl_2.2H_2O$, 0.1 mM NMDA, 0.1 mM Glycine, 118 mM NaCl, 4.7 mM KCl, 30.9 mM Glucose monohydrate and 20 mM HEPES. pH adjusted to 7.4 with NaOH) was added to the membrane preparation to depolarize the synaptoneurosomes and activate the calcium flux (Addition was done using auto-injectors). The addition of NMDA (0.1 mM) and Gly (0.1 mM) resulted in activation of NMDAR mediated calcium flux. Experiments were repeated three times on different tissue preparations with three determinations in each replicate.

4.3.2.8. Percentage inhibition calculations. The data obtained from the fluorescent readings of each well were expressed in the form of a ratio (340 nm reading/380 nm reading). This ratio indicated the net movement of Ca^{2+} ions across the membrane as it represents the ratio between unbound-Ca^{2+} and Ca^{2+}-bound to Fura-2 AM. The average ratio over a 10 s interval after 1 min of stimulation was then subtracted from the average ratio of over the last 10 s interval to give the net change in Ca^{2+} movement (Nc) across the membrane over the 5 min period. This calculation was performed for each individual well and the averages of wells containing the same test compound were calculated (Nc_{Ave}). These averages were used to calculate the percentage inhibition of the test compounds relative to the control by use of the following equation:

$$\%\,\text{inhibition} = [Nc_{Ave}(\text{Control}) - Nc_{Ave}(\text{Test compound})] \times /Nc_{Ave}(\text{Control}) \times 100\,\% \quad (2)$$

4.4. Monoamine oxidase B inhibition assay

The mitochondrial fraction of baboon liver tissue, as source of the MAO-B enzyme, was isolated as described previously by Salach & Wyler, 1987 [46], and stored at −70 °C. Following addition of an equal volume of sodium phosphate buffer (100 mM, pH 7.4) containing glycerol (50%, w/v) to the mitochondrial isolate, the protein concentration was determined by the method of Bradford using bovine serum albumin as reference standard [47]. In the current study, MMTP ($K_m = 68.3 \pm 1.60$ μM for baboon liver MAO-B) served as substrate for the inhibition studies.

The enzymatic reactions were conducted in sodium phosphate buffer (100 mM, pH 7.4) and contained MMTP (50 μM), the mitochondrial isolate (0.15 mg protein/mL) and various concentrations of the test compounds, spanning at least three orders of magnitude (0.3–300 μM). The concentration of the test compounds used in this study were 0.3 μM, 1 μM, 3 μM, 10 μM, 30 μM, 100 μM and 300 μM. The final volume of the incubations was 500 μL. The stock solutions of the inhibitors were prepared in DMSO and were added to the incubation mixtures to yield a final DMSO concentration of 4% (v/v) as concentrations higher than 4% are reported to inhibit MAO-B [48]. The reactions were incubated at 37 °C for 10 min and then terminated by the addition of 10 μL perchloric acid (70%). The samples were centrifuged at 16 000 g for 10 min, and the concentrations of the MAO-B generated product, $MMDP^+$ [49], were measured spectrophotometrically at 420 nm ($\varepsilon = 25\,000\ M^{-1}$) in the supernatant fractions.

The enzyme inhibition activities of the test compounds were determined using Equation (2) to calculate the inhibition potencies of the compounds. These potencies are expressed as percentage inhibition (% inh) of the enzyme. In determining these values, the concentration of $MMDP^+$ produced in the absence of a test compound (C_0) and the concentration of $MMDP^+$ produced by MAO-B in the presence of a maximal concentration of the test compound (C_{300}) were utilised. All determinations were conducted in duplicate, yielding the percentage inhibition as an average of the two sets of data.

$$\%\,\text{inhibition} = 100 - [(C_{300} \times 100)/C_0] \quad (3)$$

4.5. Molecular modelling

Computer-assisted docking were carried out using the CHARMm force field and the human MAO-B crystal structure (PDB ID: 2V5Z) [37], which were recovered from the Brookhaven Protein

Database (www.rcsb.org/pdb). Docking simulations were performed on the synthesised compounds (**9**–**16**) using Molecular Operating Environment (MOE) [36] with the following protocol. (1) Enzyme structures were checked for missing atoms, bonds and contacts. (2) Hydrogen atoms were added to the enzyme structure. Bound ligands were manually deleted and the ordered water molecules including 58W and 47W retained (important for the formation of a triad [Lys–H_2O–flavin N(5)] and the hydrophilic section required for recognition and directionality of the substrate amine functionality) [50] as seen with safinamide (Fig. 4). (3) The ligand molecules were constructed using the builder module and were energy minimized. (4) The active site was generated using the MOE-Alpha Site Finder. (5) Ligands were docked within the MAO-B active site using MOEDock with simulated annealing utilised as the search protocol and CHARMm molecular mechanics force field. (6) The lowest energy conformation of the docked ligand complex was selected and subjected to a further energy minimization using CHARMm force field with all possible bond rotations and chiralities explored. To determine the accuracy of this docking protocol, the co-crystallised ligand, safinamide (PDB ID: 2V5Z), was re-docked into the MAO-B active site. This procedure was repeated three times and the best ranked solutions of safinamide exhibited an RMSD value of 1.34 Å from the position of the co-crystallised ligand. In general, RMSD values smaller than 2.0 Å generally indicate that the docking protocol is capable of accurately predicting the binding orientation of the co-crystallised ligand [50,51]. This protocol was thus deemed to be suitable for the docking of inhibitors into the active site model of MAO-B.

Acknowledgements

We are grateful to the North-West University, University of the Western Cape, Medical Research Council of South Africa and the National Research Foundation of South Africa for financial support.

Appendix A. Supplementary data

Supplementary data related to this article can be found at http://dx.doi.org/10.1016/j.ejmech.2014.04.039

References

[1] H.P. Rang, M.M. Dale, J.M. Ritter, Rang and Dale's Pharmacology, Elsevier, Philadelphia, 2007, p. 508 (Chapter 35).
[2] T. Araki, T. Kumagai, K. Tanaka, M. Matsubara, H. Kato, Y. Itoyama, Y. Imai, Brain: A Journal of Neurology 918 (2001) 176.
[3] (a) T. Alexi, C.V. Borlongan, R.L.M. Faull, C.E. Williams, R.G. Clark, P.D. Gluckman, P.D. Gluckman, P.E. Huges, Progress in Neurobiology 60 (2000) 409;
(b) J.G. Greene, J.T. Greenamyre, Progress in Neurobiology 48 (1996) 613.
[4] J.U. Schweichel, H.J. Merker, Teratology 7 (1973) 253.
[5] M.P. Mattson, Nature Reviews 1 (2000) 120.
[6] N.J. Holbrook, G.R. Martin, R.A. Lockshin (Eds.), Cellular Aging and Cell Death, Wiley–Liss, New York, 1996, p. 319.
[7] A.H. Wyllie, J.F.R. Kerr, A.R. Currie, International Review of Cytology 68 (1980) 251.
[8] M. Arundine, M. Tymianski, Molecular mechanisms of calcium-dependent neurodegeneration in excitotoxicity, Cell Calcium 34 (4–5) (2013) 325.
[9] M. Arundine, M. Tymianski, Cellular and Molecular Life Sciences: CMLS 61 (2004) 657.
[10] W.J. Geldenhuys, S.F. Malan, T. Murugensan, C.J. Van der Schyf, J.R. Bloomquist, Bioorganic & Medicinal Chemistry 12 (2004) 1799.
[11] M.B. Youdim, G.G. Collins, M. Sandler, A.B. Bevan Jones, C.M. Pare, W.J. Nicholson, Nature 236 (1972) 225.
[12] G.G. Collins, M. Sandler, E.D. Williams, M.B. Youdim, Nature 225 (1970) 817.
[13] D.A. Di Monte, L.E. DeLanney, I. Irwin, J.E. Royland, P. Chan, M.W. Jakowec, J.W. Langston, Brain Research 738 (1996) 53.
[14] J.P. Finberg, J. Wang, K. Bankiewich, J. Harvey-White, I.J. Kopin, D.S. Goldstein, Journal of Neural Transmission Supplement 52 (1998) 279.
[15] M.B.H. Youdim, Y.S. Bakhle, British Journal of Pharmacology 147 (2006) S287.
[16] A. Nicotra, F. Pierucci, H. Parvez, O. Senatori, Neurotoxicology 25 (2004) 155.
[17] J.S. Fowler, N.D. Volkow, G.J. Wang, J. Logan, N. Pappas, C. Shea, R. MacGregor, Neurobiology of Aging 18 (1997) 431.
[18] B. Karolewicz, V. Klimek, H. Zhu, K. Szebeni, E. Nail, C.A. Stockmeier, L. Johnson, G.A. Ordway, Brain Research 1043 (2005) 57.
[19] J.J. Chen, D.M. Swope, K. Dashtipour, Clinical Therapeutics 9 (2007) 1825.
[20] O. Bar-Am, O. Weinreb, T. Amit, M.B.H. Youdim, FASEB 19 (2005) 1899.
[21] P.H. Yu, B.A. Davis, A.A. Boulton, Journal of Medicinal Chemistry 35 (1992) 3705.
[22] S. Mandel, O. Weinreb, T. Amit, M.B.H. Youdim, Brain. Research Reviews 48 (2005) 379.
[23] J. Joubert, W.J. Geldenhuys, C.J. Van der Schyf, D.W. Oliver, H.G. Kruger, T. Govender, S.F. Malan, Chemmedchem 7 (2012) 375.
[24] J. Zah, G. Terre'blanche, E. Erasmus, S.F. Malan, Bioorganic & Medicinal Chemistry 11 (2003) 3569.
[25] K.B. Brookes, P.W. Hickmott, K.K. Jutle, C.A. Schreyer, SAJC 45 (1992) 8.
[26] J. Joubert, S. Van Dyk, I.R. Green, S.F. Malan, Bioorganic & Medicinal Chemistry 19 (2011) 3935.
[27] J. Joubert, S. Van Dyk, I.R. Green, S.F. Malan, European Journal of Medicinal Chemistry 46 (2011) 5010.
[28] H.J.R. Lemmer, J. Joubert, S. van Dyk, F.H. van der Westhuizen, S.F. Malan, Medicinal Chemistry. [Medicinal Chemistry (Shariqah (United Arab Emirates))] 8 (2012) 361.
[29] J. Joubert, H. Samsodien, Q.R. Baber, D.L. Cruickshank, M.R. Caira, S.F. Malan, Journal of Chemical Crystallography 44 (2014) 194.
[30] Mitochondrial Membrane Potential Disruption Assay. DePsipher™ assay kit. http://www.rndsystems.com/product_detail_objectname_mitochondrial_membrane_disruption.aspx (accessed 31.03.14.).
[31] C.J. Van der Schyf, G.J. Squier, W.A. Coetzee, Pharmacological Research Communications 18 (1986) 407.
[32] E.B. Hollingsworth, E.T. McNeal, J.L. Burton, R.J. Williams, J.W. Daly, C.R. Creveling, The Journal of Neuroscience: The Official Journal of the Society for Neuroscience 5 (1985) 2240.
[33] J.J. Van der Walt, C.J. Van der Schyf, J.M. Van Rooyen, J. De Jager, M.N. Van Aarde, South African Journal of Science 84 (1988) 448–450.
[34] A.E. Medvedev, A.S. Ivanov, N.S. Kamyshanskaya, A.Z. Kirkel, T.A. Moskvitina, V.Z. Gorkin, N.Y. Li, V.Y. Marshakov, Journal of. Biochemistry and Molecular Biology 36 (1995) 113.
[35] J.P. Petzer, N.C. Castagnoli, M.A. Schwarzschild, J. Chen, C. Van der Schyf, Journal of Neurotherapy 6 (2009) 141.
[36] Molecular Operating Environment (MOE), Version 2011.10. http//www.chemcomp.com.
[37] C. Binda, J. Wang, L. Pisani, C. Caccia, A. Carotti, P. Salvati, D.E. Edmondson, A. Mattevi, Journal of Medicinal Chemistry 50 (2007) 5848.
[38] Y. Tsugeno, I. Hirashiki, F. Ogata, A. Ito, Journal of Biochemistry 118 (1995) 974–980.
[39] A.L. Maycock, R.H. Abeles, J.I. Salach, T.P. Singer, Biochemistry 15 (1976) 114.
[40] D.J. Mitchell, D. Nikolic, E. Rivera, S.O. Sablin, S. Choi, R.B. van Breemen, T.P. Singer, R.B. Silverman, Biochemistry 40 (2001) 5447.
[41] R.C. Cookson, E. Crundwell, R.R. Hill, J. Hudec, Chemistry and Industry (1958) 1003.
[42] A.P. Marchand, S.C. Suril, A.D. Earlywine, D.R. Powell, D. Van der Helm, The Journal of Organic Chemistry 49 (1984) 670.
[43] T.G. Dekker, D.W. Oliver, SAJC 32 (1979) 45.
[44] (a) S.J. Benavide, Y. Claustre, B. Scatton, The Journal of Neuroscience: the Official Journal of the Society for Neuroscience 8 (1988) 3607;
(b) W.J. Geldenhuys, S.F. Malan, J.R. Bloomquist, C.J. Van der Schyf, Bioorganic & Medicinal Chemistry 15 (2007) 1525;
(c) K. Resch, W. Imm, E. Ferber, D.F.H. Wallach, H. Fischer, Die Naturwissenschaften 58 (1971) 220;
(d) A.K. Stout, I. Reynolds, The Journal of Neuroscience: the Official Journal of the Society for Neuroscience 89 (1999) 91.
[45] E.B. Hollingsworth, E.T. McNeal, J.L. Burton, R.J. Williams, J.W. Daly, C.R. Creveling, The Journal of Neuroscience: the Official Journal of the Society for Neuroscience 5 (1985) 2240.
[46] J.I. Salach, W. Weyler, Methods in Enzymology 142 (1987) 627.
[47] M.M. Bradford, Analytical Biochemistry 72 (1976) 248.
[48] C. Gnerre, M. Catto, F. Leonetti, P. Weber, P.A. Carrupt, C. Altomare, A. Carotti, B.J. Testa, Journal of Medicinal Chemistry 43 (2000) 4747.
[49] H. Inoue, K. Castagnoli, C.J. Van der Schyf, S. Mabic, K. Igarashi, N. Castagnoli, Journal of Pharmacology and Experimental Therapeutics 291 (1999) 856.
[50] C. Binda, M. Li, F. Hubalek, N. Restelli, D.E. Edmondson, A. Mattevi, PNAS 100 (2003) 9753.
[51] J. Boström, J.R. Greenwood, J. Gottfries, Journal of Molecular Graphics & Modelling 21 (2003) 449.